

# Determining Optimum Wet Milling and Leaching Parameters for Maximum Recovery of Gold

<sup>1</sup>Nkosikhona Hlabangana, <sup>2</sup>Nonhlanhla G. Mguni, <sup>3</sup>Siboniwe Bhebhe,  
<sup>4</sup>Gwiranai Danha, <sup>5</sup>Joel Tshuma

<sup>1,2,3,5</sup>Department of Chemical Engineering National University of Science and Technology P O Box AC 939  
Ascot Bulawayo Zimbabwe

<sup>4</sup>Department of Chemical, Materials and Metallurgical Engineering, College of Engineering and Technology, Botswana  
International University of Science and Technology, Plot 10071 Boseja Ward, Private Bag 16 Palapye, Botswana.

---

**Abstract:** The comminution and leaching unit operations play a vital role in the extraction process of valuable minerals from ores. Historical research efforts have focused more on optimizing these two unit operations individually rather than as an entire integrated process. The approach employed in modern day research is now driven by the process intensification philosophy. Process intensification detects that developing an integrated approach to mineral processing systems and flow sheets leads to improved efficiency of the overall process and can help attain optimum recovery and a reduction in energy and material costs. In this article, we present laboratory scale batch grinding and leaching profiles of a mono-sized gold ore sample (-1700 + 850  $\mu\text{m}$ ). The sample was obtained from a run-of-mine (ROM) ore of one of the leading gold processing plants in South Africa. Various combinations of grinding media fill level and ball size were investigated, showing that breakage is more pronounced for the larger ball sizes tested. We also found that using a higher media filling ( $J = 30\%$ ) and a larger media size (30 mm) consumed more energy with less gold recovered during a 24 hour leaching period, compared to when a smaller  $J$  of 15% and 20 mm media was used. Our results show that efficient application of energy is vital and maximum profit is a complex function of energy usage and particle size.

**Keywords:** gold, Historical research, mineral processing, energy, material costs.

---

## 1. INTRODUCTION

The comminution unit operation in the beneficiation of gold ores is a significant process carried out where ore particles are gradually reduced in size in order to produce material of the size class of interest with varying degrees of liberation. This is done so as to expose or liberate the gold value metal from gangue material. The liberated value mineral is then subsequently recovered by a downstream leaching unit operation. The two processes, namely: comminution and leaching, are energy and cost intensive, constituting the major overall costs in a typical gold plant. Therefore, efforts that may result in even a small increase in the processing efficiency of the ore are most welcome as they will have a large impact on the overall operating costs of the plant.

In this article, our objective is to determine the trade-off between the additional gold recoveries achievable as a function of reduced particle size, versus the energy costs incurred in producing the reduced particle size. To that end, we also simulated the power drawn by the ball mill using the Discrete Element Method (DEM) approach.

### 1.1 Prediction of mill power:

The power drawn by a mill during batch test experimental runs is of paramount importance in comminution as it relates the energy input to the size reduction process. The common power prediction methods involve analytically determining the net power taking into consideration the internal dynamics of the tumbling mill. A number of tools have been introduced to help determine or calculate the power drawn by a mill. The DEM tool has found its usefulness in the mineral processing industry and is now widely used in predicting this power.

The DEM technique was first introduced by Cundall and Strack (1979) as a mathematical approach used to simulate the interactions of deformable spheres and used extensively to study the general flow behavior within a tumbling ball mill environment, and in particular power draw (Djordjevic, 2003). The DEM can simulate the dynamic interaction of particles in any environment and has the advantage of being independent of results of previous test work. This modelling tool predicts the dynamics of charge motion for individual particles and is able to calculate stresses and forces between the particles. Combining such information with the strength of particle distribution data and load holdup estimations the prediction of the rates of breakage of different size fractions is made possible. In addition, the energy of each collision can be used to determine the overall power consumed by the mill as a function of various operational conditions.

### 1.2 The milling kinetics:

The milling kinetics have always been based on a population balance model (Austin 1972) that helps in determining the breakage and selection functions. The PBM (Equation 1) assumes first order breakage kinetics.

$$\frac{dw_i(t)}{dt} = -S_i w_i(t) + \sum_{j=1}^{i-1} b_{i,j} S_j w_j(t) \quad (1)$$

Breakage in top size material is then expressed as:

$$\frac{dw_i}{dt} = -S_i w_i(t) \quad (2)$$

Assuming  $S_i$  does not change with time (for normal breakage) on integrating the Equation 2 leads to:

$$\log w_i(t) - \log w_i(0) = -S_i t / 2.3 \quad (3)$$

Where:  $w_i(t)$  is the weight fraction of the mill hold-up that is of size  $i$  at time  $t$ .

Plotting  $\log w_i(t)$  against  $t$  yields a linear relationship if the grinding process follows a first order breakage model. If there are any deviations from first order it means breakage rates are either slowing down or accelerating of breakage rates. When grinding feed material in the mill, various daughter particle sizes are produced. The breakage distribution function  $b_{i,j}$  that accounts for material breaking into size  $i$  from some upper particle size  $j$  is expressed as:

$$b_{i,j} = \frac{\text{mass of particles from class } j \text{ broken to size } i}{\text{mass of particles of class } j \text{ broken}} \quad \text{where } i < j \quad (4)$$

The cumulative breakage function is a convenient term for modelling and is related to  $b_{i,j}$  as follows :

$$B_{ij} = \sum b_{ij} \quad (5)$$

$B_{ij}$  is a sum given by fractions of material passing the upper screen size of  $i$  obtained from primary breakage of size  $j$  material. For a normalisable material, Austin (1984) further proposed a cumulative breakage function model given as:

$$B_{i,j} = \Phi_j \left( \frac{x_{i-1}}{x_j} \right)^\gamma + \left( 1 - \Phi_j \right) \left( \frac{x_{i-1}}{x_j} \right)^\beta \quad n \geq i \geq j \geq 1 \quad (6)$$

Where  $\beta, \gamma, \Phi$ , and  $\delta$ , are material dependent model parameters.

### 1.3 The Integrated milling and leaching process

After the comminution unit process, the ground material is reacted in an oxygenated cyanide solution that dissolves the gold, leaving solid gangue minerals that are disposed of. The effect of particle liberation is very important in gold leaching. Studies have shown that grinding finer yields high recoveries (de Andrea Lima and Houdon, 2005). While it is accepted that a finer size distribution is favorable for increased gold recovery, the benefits of the increased recovery could be offset by higher grinding costs and cyanide consumption (Breuer, 2008). A finer particle size accords the leach reagents better access to the gold material, which leads to an increase in cyanide consumption.

An integrated process of the grinding and cyanide leaching may provide a tool to identify the optimum size distribution for processing a gold ore and to study various flow sheet configurations, such as separate leaching of coarse and fine particles (Gagnon, 2009).

The rationale behind this joint optimization approach is that the optimization of a single unit does not always coincide with the optimum for the whole process. In leaching, particle size or degree of liberation will play a major factor on the dissolution rate hence the number of reactor vessels required for the leaching. Therefore when optimizing a joint leaching and comminution process, a tradeoff must be struck in terms of degree of liberation so that expenses associated with both comminution and leaching are kept minimal.

## 2. MATERIAL AND METHOD

### 2.1 Mill and feed material characteristics:

We obtained the material for our test runs from the run-of-mine of the Witwatersrand gold mine in South Africa. After sample preparation, we crushed the ore in a jaw and cone crusher and classified it into different size fractions by using a standard sieving procedure. We then isolated material from the  $-1700 + 850 \mu\text{m}$  size range and accumulated it as we were going to use it as our feed material.

The mill shown in Figure 1 was used for our experimental programme. The mill speed was controlled through an electronic speed meter that enabled one to set and adjust the motor speed. The power of the mill can be measured through an instrument comprising of a load beam, which converts the force exerted onto it into a corresponding voltage. One of the ends of the load beam was attached to a rod, which is turned by the rotation of the mill.

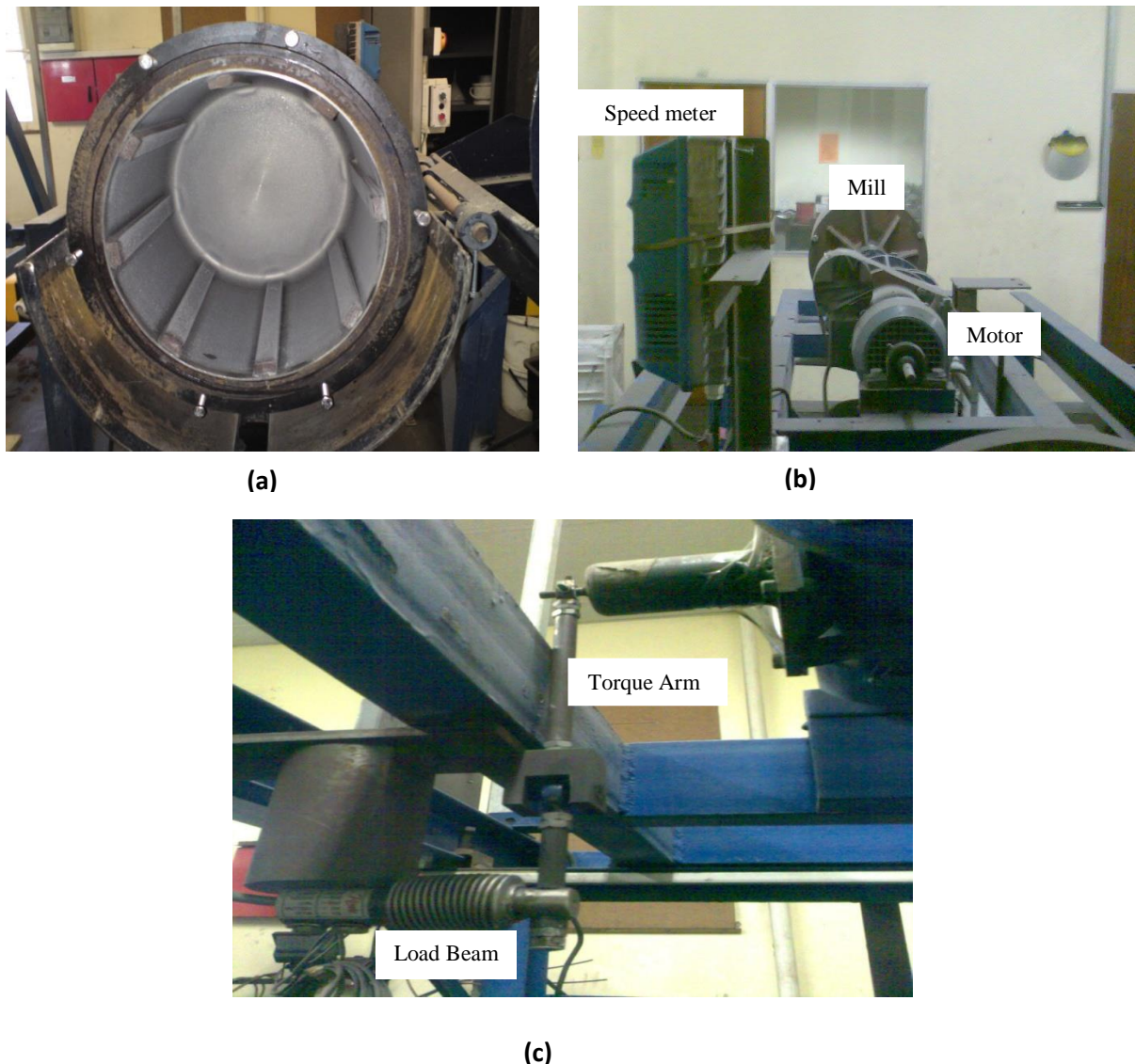


Fig. 1: (a) The front and rear view of the mill (b) Calibration section of the mill equipment (Katubilwa, 2012).

The first batch of our experiments was aimed at estimating the selection and breakage functions of the gold ore. To that effect, four mono-size fractions (-1700+1180; -1180+850; -850+600 and -600+425  $\mu\text{m}$ ) were prepared and then batch milled for different time intervals in a laboratory ball mill in order to determine the selection function. More samples were later also milled using the conditions as stipulated in Table 1 and 2 in order to calculate the breakage functions. The mill products were then analyzed for product size distribution using the standard dry sieving technique.

**Table 1: Conditions for milling kinetics experiments with varying U (Interstitial filling)**

|            |                            |                 |       |      |       |
|------------|----------------------------|-----------------|-------|------|-------|
| Mill speed | Operational                | 75% of critical |       |      |       |
| Balls      | Diameter                   | 20mm            |       |      |       |
|            | Bed porosity               | 40%             |       |      |       |
|            | Ball filling volume, J%    | 5%              |       |      |       |
| Feed       | Size ( $\mu\text{m}$ )     | -1700+850       |       |      |       |
|            | Interstitial filling (U %) | 50              | 75    | 100  | 175   |
|            | Powder filling ( $f_c$ )   | 0.01            | 0.015 | 0.02 | 0.035 |

**Table 2: Conditions for milling kinetics experiments on varying J (ball filling) on milled material**

| Run Number | J (%) | $d_m$ (mm) | Mass of powder (kg) | Mass of media (kg) | Volume of water (ml) |
|------------|-------|------------|---------------------|--------------------|----------------------|
| 1          | 5     | 10         | 0.491               | 4.697              | 163.67               |
| 2          | 5     | 20         | 0.491               | 4.697              | 163.67               |
| 3          | 15    | 10         | 1.474               | 14.091             | 491.01               |
| 4          | 15    | 20         | 1.474               | 14.091             | 491.01               |
| 5          | 30    | 30         | 2.946               | 28.182             | 982.02               |

More tests were done according to the conditions specified in Table 1 using the ball size, media and charge filling shown in Table 2. The measured feed material (-1700+850  $\mu\text{m}$ ), media and water were loaded into the mill and milled for 3 minutes. The mill was stopped and its contents emptied and stored in a bucket. Four more grinding times were used per run and these were 5, 15, 30 and 60 minutes. The slurry obtained after each grinding time was filtered using a Buchner filter and the residue material was then dried in an oven set at 60 °C for 4 hours. The product from the oven was then taken for particle size analysis using a standard dry sieving technique.

## 2.2 The Leaching procedure:

Standard bottle rolling leach tests were performed on 200 grams samples from each size class shown in Table 3. The gold ore was suspended in 200 ml of distilled water to which lime was added so as to ensure that the pH of the pulp was above 11 in order to avoid the production of poisonous hydrogen cyanide (HCN). Individual leach bottles containing the ore sample, distilled water and lime were then conditioned on a roller for about an hour before adding 0.06 grams of sodium cyanide at the start of each leach. The bottle rolling tests were all carried out on a bottle roller under ambient conditions. The leach tests were carried out for 1, 2, 3, 5 and 24 hours on material from each of the selected size classes. The leach bottles were removed from the bottle roller after the completion of each leach, whereupon they were filtered on a Buchner funnel to remove the leach liquor. The leach liquor was re-filtered on a Millipore filter before gold analysis using an Atomic Adsorption Spectrometer. The solid residues are dried and a sample is taken to have a head assay of the material.

Table 3: Particle size classes used for the leaching experiments

| Size class | Upper (microns) | Lower (microns) |
|------------|-----------------|-----------------|
| M1         | -1700           | +850            |
| M2         | -850            | +300            |
| M3         | -300            | +150            |
| M4         | -150            | +75             |
| M5         | -75             | +25             |
| M6         | -25             | to pan          |

### 3. RESULTS AND DISCUSSION

#### 3.1 Milling results:

##### 3.1.1 Calculation of S function from four monosize fractions:

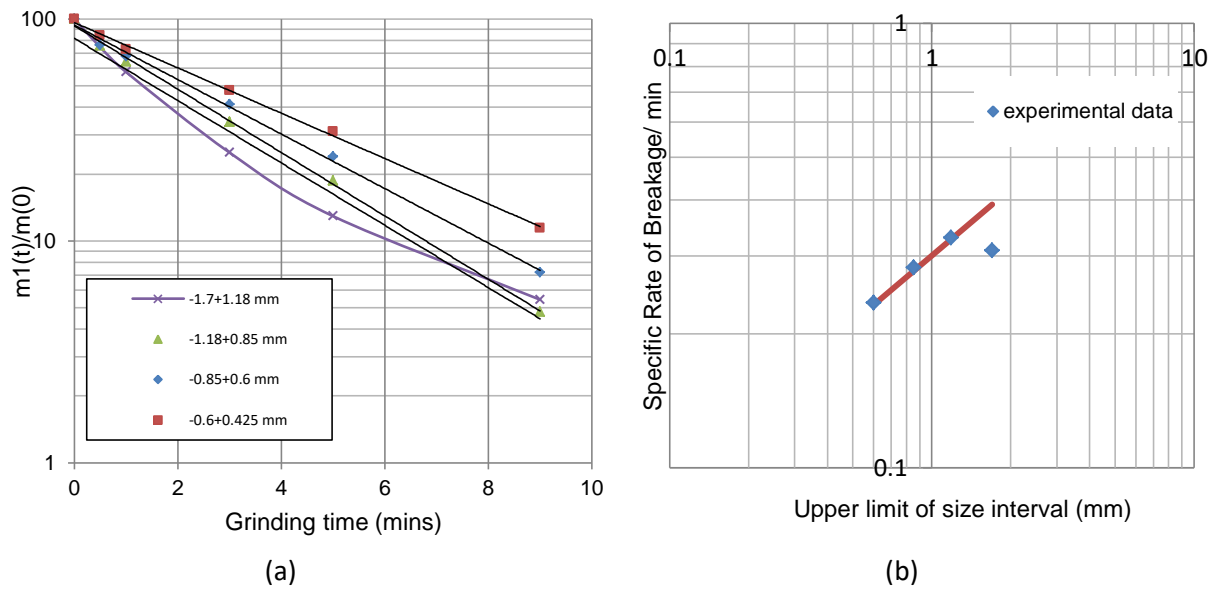


Fig. 2: (a) First-order plots for different feed classes milled (b) Variation of  $S_i$  with particle size

Fig. (2a) shows the first-order line graphs for different feed sizes of gold ore. The results show that milling of fine size classes follows first-order breakage. However, the coarse size fraction (1700-1180 $\mu$ m) showed deviation from it. This probably could be attributed to fact that breakage in the region is termed ‘abnormal’ where ore particles are too large and cannot be sufficiently nipped by the steel balls.

Table 4: Selection function values for different feed size classes

| Mono-sized Gold ore material | Selection function value |
|------------------------------|--------------------------|
| -1700+1180 $\mu$ m (S1)      | 0.3230                   |
| -1180+ $\mu$ m 850 (S2)      | 0.3286                   |
| -850+600 $\mu$ m (S3)        | 0.2827                   |
| -600+425 $\mu$ m (S4)        | 0.2351                   |

The  $S_i$  values of each monosize fractions that displayed first-order behavior were obtained from the gradient of the line graph. The selection function values in Table 4 were plotted against particle size the graph obtained shows there is a linear relationship between  $S_i$  and particle size for particle sizes less than ~1200 $\mu$ m. Breakage is assumed to be normal for the 20 mm balls until a peak value is reached and thereafter it decreases as particle size is increased. Using a power function the parameter alpha ( $\alpha$ ) was calculated to be 0.5 (Fig. 2(b)).

3.1.2 Calculation of the breakage function parameters:

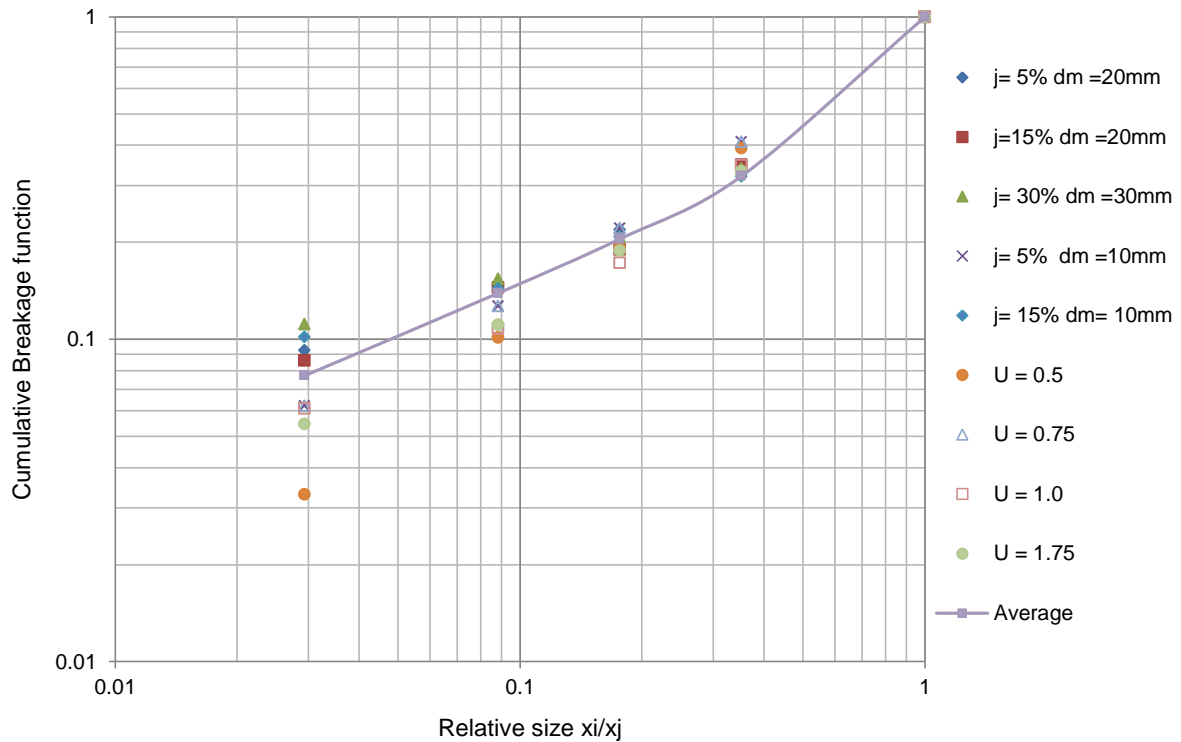


Fig. 3: Plot of breakage function values against feed size

By definition, these values are to be calculated from the PSDs at short milling times, resulting in 20 - 30% of ore particles broken out of the top size class. The BII method [5] was used to determine the breakage parameters, and these are shown as graphical representation in Figure 3. The diagram shows the primary breakage distribution plots for 10 mm, 20 mm, 30 mm media and different U values.

The  $B_{ij}$  values obtained were fitted to the model in Equation 7 which allowed the breakage function parameters for the gold ore to be calculated. For all the media sizes and feed condition used, the average breakage function parameters determined were  $\beta = 3.6$ ,  $\gamma = 0.5$  and  $\Phi = 0.68$ . Average  $B$  values were calculated because these do not depend on milling conditions as confirmed by experiments.

Table 5: Results for calculated and measured power values

| Test Condition | Power (Watts) |          |
|----------------|---------------|----------|
|                | DEM           | MEASURED |
| J=5% dm=10mm   | 13.79         | 11.63    |
| J=5% dm= 20mm  | 9.98          | 9.539    |
| J=15% dm=10mm  | 48.61         | 44.94    |
| J= 15% dm=20mm | 37.42         | 35.52    |
| J= 30% dm=30mm | 80.99         | 75.081   |

The power measured experimentally and that obtained through DEM simulations of a similar system are shown in Table 5. The results show that the 10 mm balls consume more power compared to the 20 mm. The power draw of the 10 mm balls is about 30% more than the 20 mm media at the same conditions and increasing J from 5% to 15% for the same media size, leads to a power increase greater than 3.5 times.

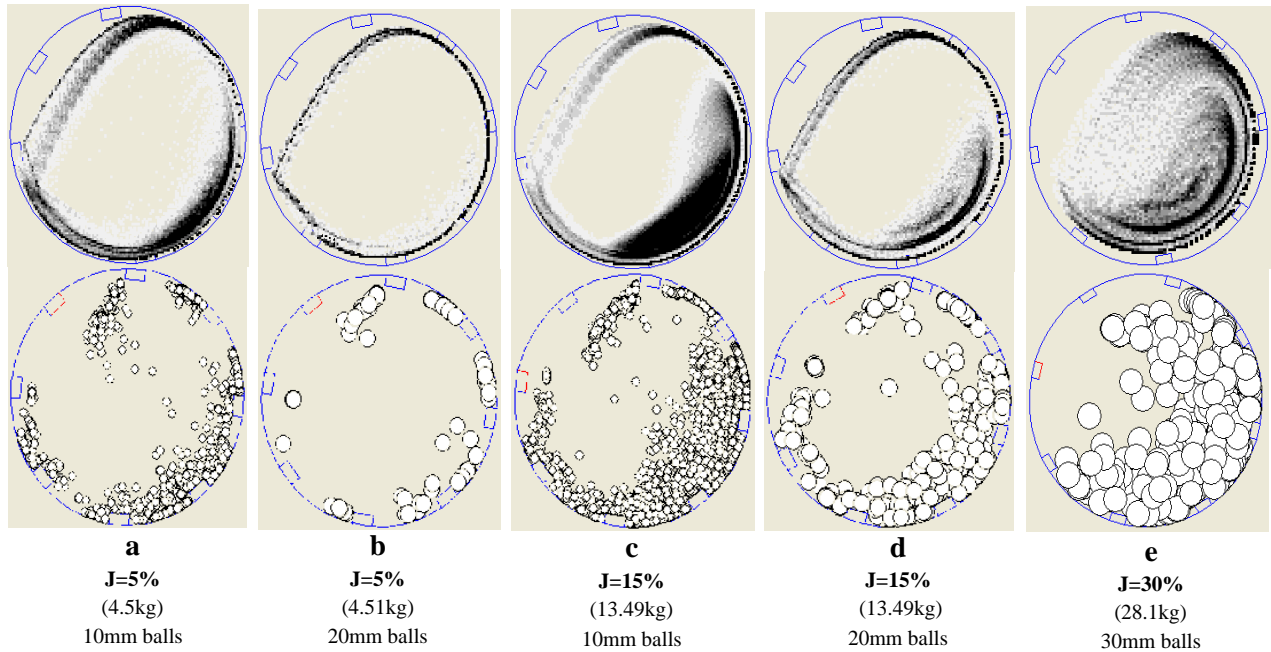


**Fig. 4: Simulated charge motion of 20.6 litre mill**

Fig. 4(a) and (c) show that the smaller 10 mm balls are lifted higher by the lifters before rolling off the liners and the mill draws more power in raising these balls. The lower height obtained by the 20 mm media in diagrams (b) and (d) explain why 20 mm balls draw less power. It is also possible that the 20 mm balls give back more kinetic energy to the mill as they fall on the toe side. Instead of the mill lifting the balls, the balls are trying to turn the mill as they fall on the toe side of the mill. In a ball mill, the power consumption varies according to the changes in the center of gravity in the internal volume of the mill. When the mill is filled with media only, the J value is higher but on adding feed the center of gravity of grinding media shifts up, the J values decrease and therefore power consumption also decreases.

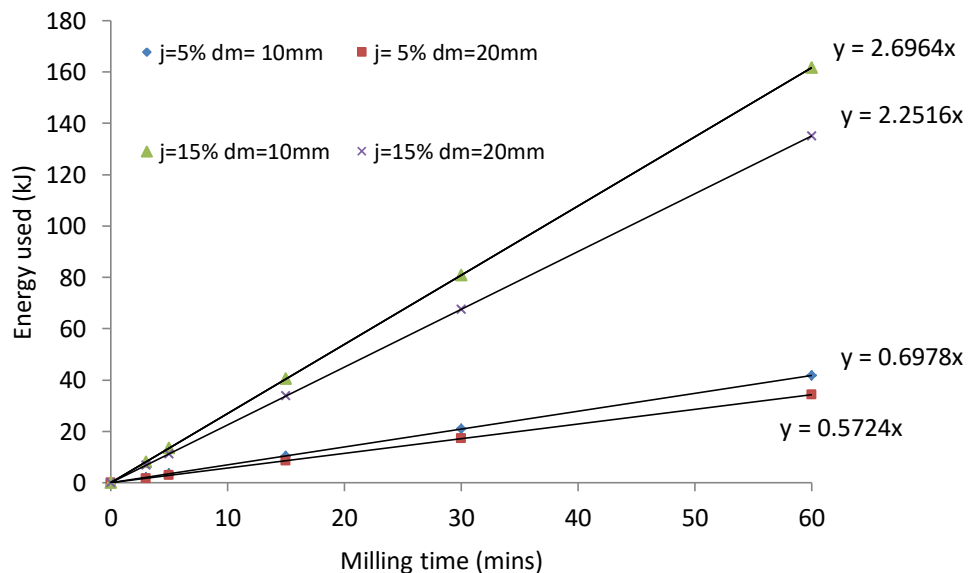


**Fig. 5: Variation of energy used with milling time**

Fig. 5 shows how the energy varies with grinding time and ball fill (J). From the results presented, total energy consumption increases as ball fill and milling time increases. Interestingly it can be seen that for both low ball filling values (J = 5% and 15%), the bigger balls draw less power than the smaller balls. This is in agreement with the results from the DEM simulations (Table 5).

3.1.3 Milling particle size distributions:

Fig. 6 gives the grinding and the cumulative passing profiles for the low J value of 5% using 10 mm media. It can be seen as the mill rotates material of size class one breaks and therefore decreases. In the intermediate classes (M2-M5), the mass initially increases then finally decreases as milling proceeds. The mass fraction of size class six is ever increasing until all the material breaks into that size class (otherwise referred to as the sink).

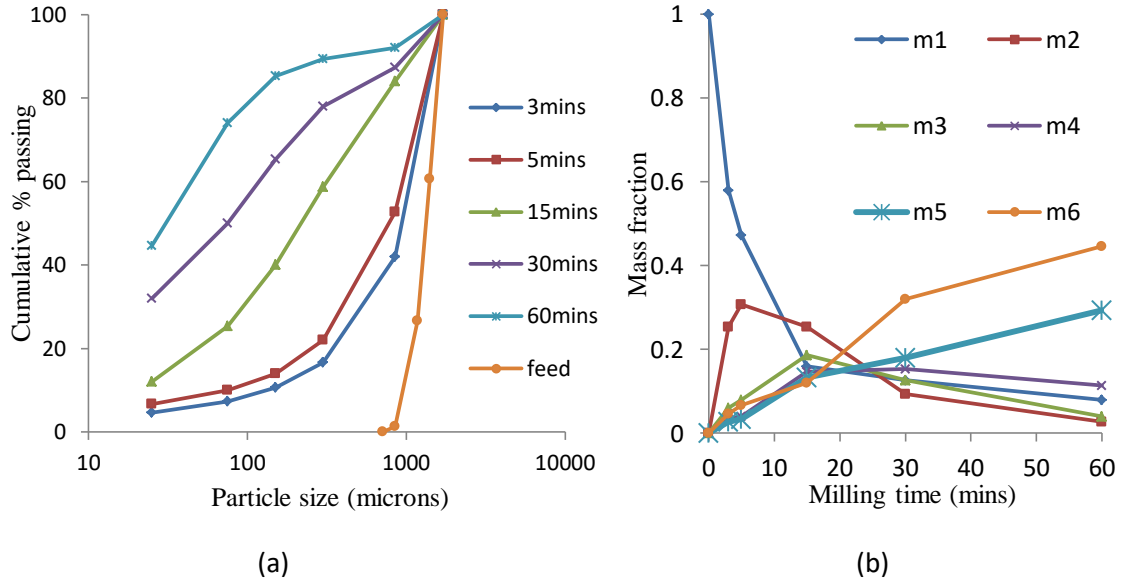


Fig. 6: Class size distribution at ( $J = 5\%$   $d_m = 10\text{mm}$ ). (a) Cumulative % passing vs. particle size and (b) grinding profiles of all six class sizes vs. time

Fig. 7 shows the particle size distributions for the  $J = 5\%$  case with the different ball sizes of 10 mm and 20 mm. As shown, the 20 mm balls are more effective in breaking material to finer size compared to the 10 mm media. The breakage may be attributed to the 20 mm ball smashing the particles to fine and medium sized particles. The 10 mm balls are good at chipping the larger particles forming more of the intermediate classes during this milling process.

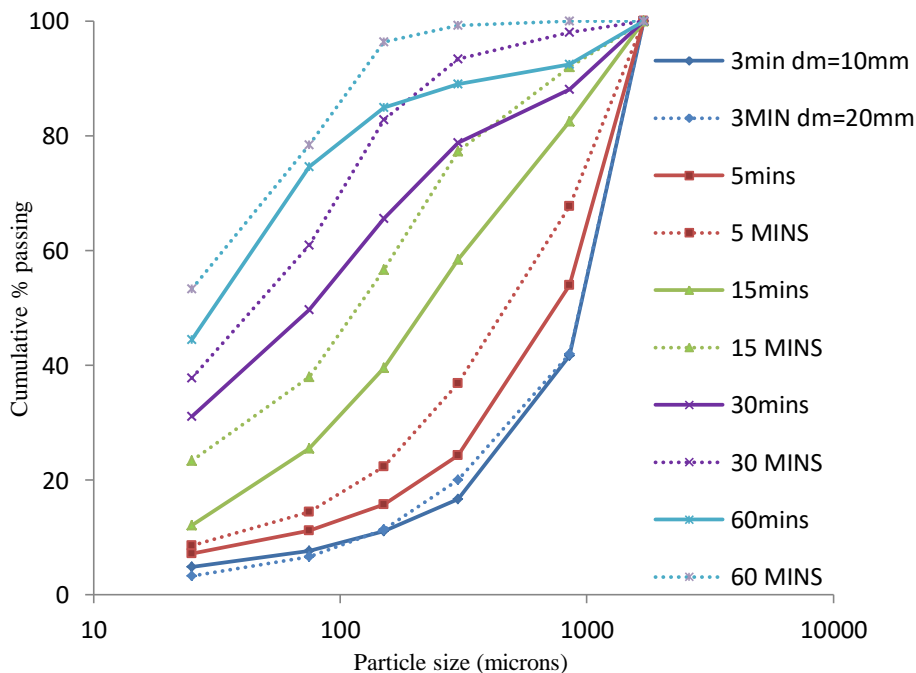


Fig. 7: Class size distribution comparisons  $J = 5\%$ . Cumulative % passing profile vs. particle size comparisons for 10 and 20 mm ball sizes



The same trend is observed for the case of  $J = 15\%$  (Figure 8). The 20 mm media is more effective in breaking the M1 size class to the smaller size classes and during the initial stages of the milling process more of M2 and M6 are formed.

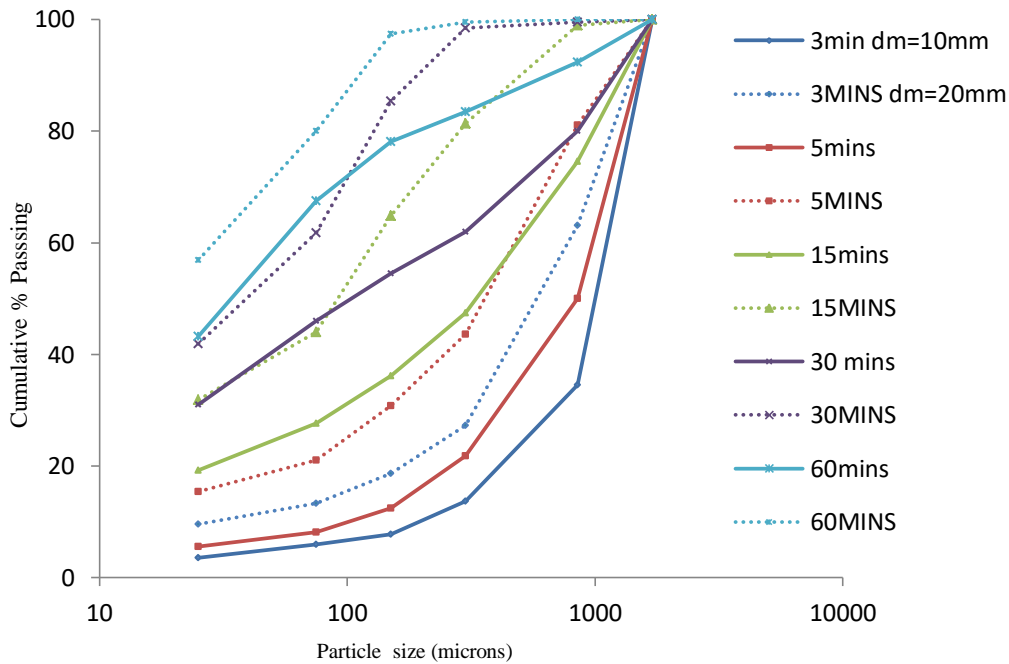


Fig. 8: Class size distribution comparisons.  $J = 15\%$ . Cumulative % passing profile vs. particle size comparisons for 10 and 20 mm ball sizes

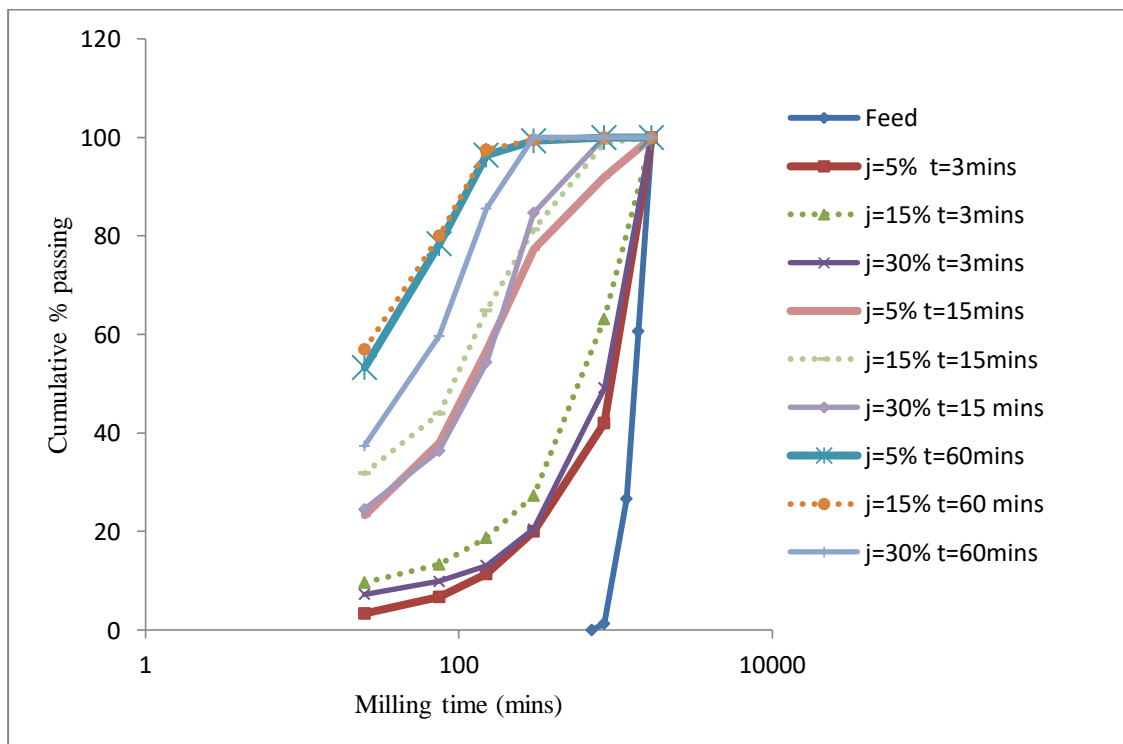
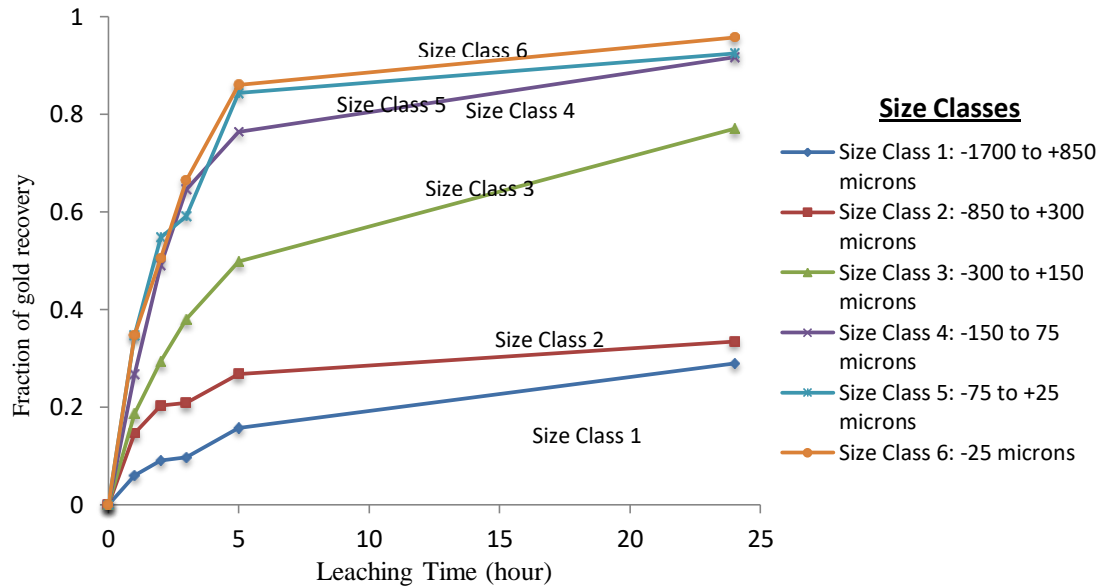


Fig. 9: Class size distribution comparisons.  $J = 5\%, 15\%$  and  $30\%$ . Cumulative % passing profile vs. particle size comparisons for 30 and 20 mm ball sizes.

Fig. 9 shows the particle size distribution for  $J = 5\%$  and  $15\%$  using the 20 mm balls and included is a high ball filling 30% with 30 mm media. It can be seen that using 30 mm balls with high ball filling is not as effective as the smaller ball fillings and smaller media. This is because there is less breakage or formation of finer material after a total milling time of 60 minutes.

**Leaching results:**

The leach curves arising from the bottle rolling test are depicted in Fig. 10. The recoveries are based on the individual size class head assays and the gold content of the leach liquor at the end of each bottle rolling test.



**Fig. 10: Leach profiles for milled size classes of a typical Witwatersrand Far West Rand Gold ore.**

For comparative purposes the bottle rolling tests were carried out to 24 hours, although actual residence times in a typical leach cascade are around 44 hours. In general, it was found that recovery increases as leaching time increases. This means in finer material (M6) the leaching reagent has better access to the valuable gold material, hence where the highest gold recovery of ~95.8% is achieved. Size class 1 has the lowest recovery of ~ 24.29% and this low value is due to value material being locked in the mineral matrix and not accessible by the leaching solution.

The total amount of gold available after a particular milling time was calculated from the % recovery, the average head grade and the mass fraction of each size class at that particular milling time. Figure 11 gives the results.

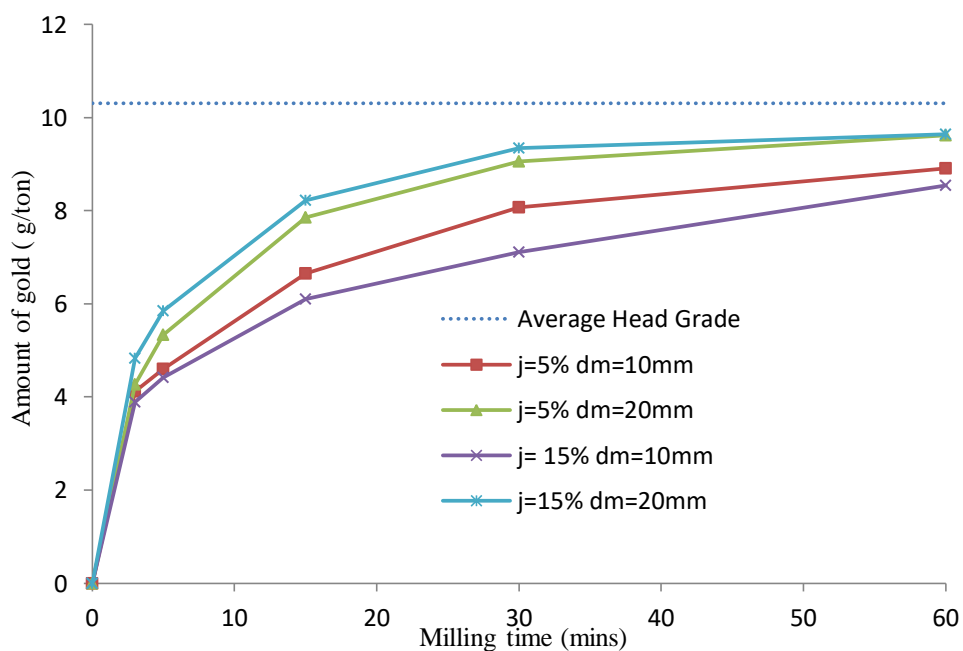


**Fig. 11: Variation in the amount of gold and milling time for 24 hour leach.**

The average head grade was found to be 10.3 g/ton ± 0.67 g/ton, from 6 measurements. Ideally, the entirety of this amount would be able to be recovered during milling and leaching. However, the leaching reagent cannot access a significant amount of gold (especially for size classes 1 and 2 – see Fig. 10), which causes the rate of leaching to be very slow and finite for an extended period of time (Crundwell and Good, 1995). The graph shows that the case of J = 15% with 10 mm media produces the least amount of gold after each particular grinding time and this can be attributed to less liberation of the gold. It can also be shown that the J = 5% and 20 mm curve takes a little longer compared to the J = 15% and 20 mm curves to reach their recovery after 24 hours of leaching. At this point the goal is to maximize the recovery of gold in the shortest amount of time, so it is recommended to operate with J = 15% and 20 mm media.

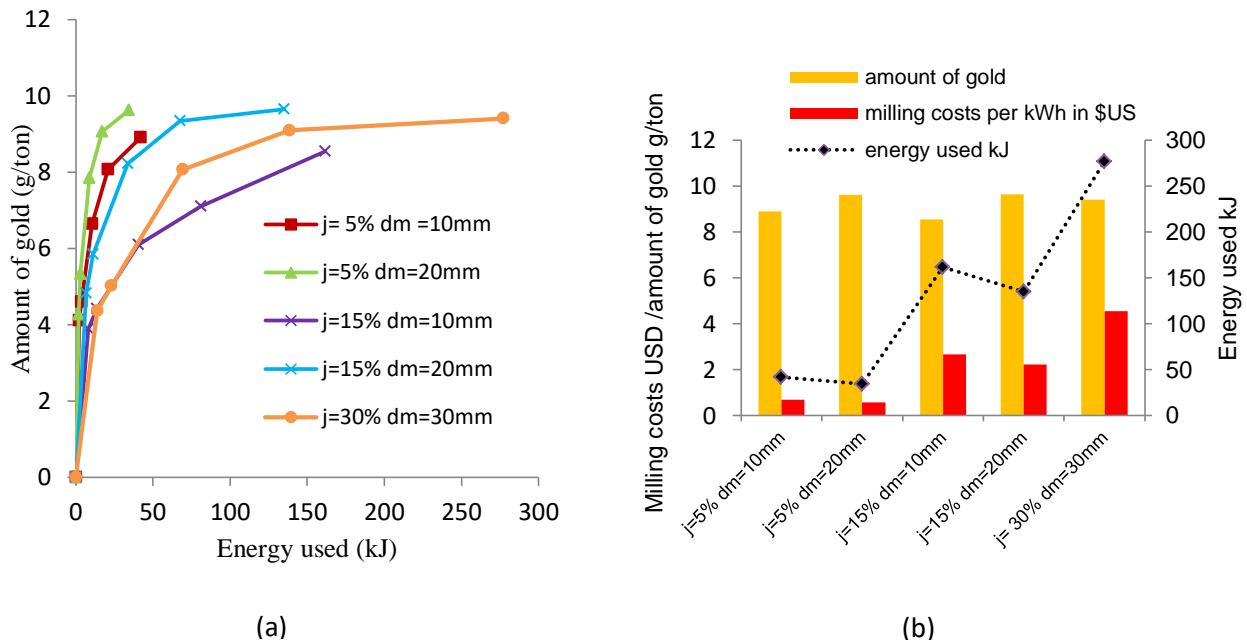


Fig. 12: (a) Variation in the amount of gold and energy used for different J and  $d_m$  values (b) Plot of milling costs USD/ amount of gold g/ton and Energy used vs. milling conditions.

A graph showing the of amount of gold obtained and energy used during the 24 hour leach period for different  $d_m$  and J values is shown in Fig. 12(a). The low J values use a low amount of energy and achieve a high amount of gold recovery. The J = 15% and  $d_m$  = 20 mm case gave the highest amount of gold recovery in less time whilst accompanied by high energy usage (compared to the J = 5% cases). The J = 15% and 10 mm media case consumes the highest amount of energy to get to about 8 g/ton of gold compared to the other combinations of media size and ball filling. Using the ball filling of 30% and 30 mm balls also achieves high amount of recovery but at a high energy consumption. achieves a high recovery, accompanied by highest energy consumption.

The best case of recovery from the milling time yielded ~9.64 g/ton of gold using ~135.09 kJ energy, which would cost ~ USD 2.2 (assuming the South African equivalent would be R50.3c per kWh or USD 0.0592 (Fig. 12(b)). The next best case was J=5% with a media size of 20 mm, which recovered 9.62 g/ton and consumed 34.34 kJ of energy.

#### 4. CONCLUSION

The study showed that 20 mm media were effective in milling for both J = 5 and 15% values with the experimental conditions used. The M6 size class (-25 $\mu$ m) gave the highest recovery of ~95.8% after a 24 hour leach. The  $d_m$  = 10mm cases produce a lower amount of gold after each particular grinding time and this can be attributed to less liberation. It can also be shown that the J = 5% and 20 mm curve takes a little longer to attain maximum gold recovery compared to the J = 15% and 20 mm curves. From the leaching curves the size class M4 (-150+75  $\mu$ m) produces recoveries comparable to the smaller size M5 (-75+25  $\mu$ m) which suggests that a milling cut-off size closer to -150  $\mu$ m could be adopted since it would mean less capital and operational expenses in the form of reduced grind time and reduced leaching reagent consumption. It was also discovered that in terms of energy, using J = 5% and 30% with 20 mm media gave high recovery of gold with less energy used after 60 minutes of milling and 24 hours leaching. In terms of overall profit the J

= 5% and 15% with the 20 mm media size provided a maximum profit of ~ \$489US per ton of feed. This proved that using lower energy at a high recovery would be ideal for an integrated leach and milling circuit. The overall main cost in the mineral processing industry is a function of time, energy and capital. A balance between these must be struck. Further work will look at modelling an integrated system and changing some of the factors like mill speed and percentage of solids and see how they affect gold recovery. In addition, the cost model will be expanded to include capital costs to reflect the decrease in leaching time for a finer grind.

#### REFERENCES

- [1] Austin, I. G., Klimpel, R. R. & Luckie, P. T. 1984. *Process engineering of size reduction: ball milling*, New York, American Institute of Mining, Metallurgical, and Petroleum Engineers, Inc.
- [2] Bond F. C.: The Third Theory of Comminution. AIME Trans.1952 vol. 193, p. 484.
- [3] Breuer, P.L., Hewitt D.M., Meak. R.L., (2008). Does pre-oxidation or lead (ii) addition reduce the impact of iron sulphides in cyanidation? *Hydrometallurgy 2008: Proceeding of the 6th International Symposium, SME, phoenix USA*, august, pp. 750-757.
- [4] Cundall, P.A. and Strack, O.D.L. (1979). A discrete numerical model for granular assemblies. *Geotechnique*. **29**(1): p. 47-65.
- [5] de Andrade Lima, L.R.P & Hodouin, D. (2005). A lumped kinetic model for gold ore cyanidation, *Hydrometallurgy*. Vol. 79 pp 121-137.
- [6] Djordjevic, N., (2003). Discrete element modeling of the influence of lifters on power draw of tumbling mills. *Minerals engineering*, **16**(4): pp 331-336.
- [7] Feurstenau, J.J, Lutch, A. de, (1999) The effect of ball size on the energy efficiency of hybrid pressure roll mill/ ball mill grinding, *power technology*. 105199-204.
- [8] Gagnon C., Landry G., Ourriban M., Pelletier P., Bouajila A., (2009). Implementation of cyanidation by size class at sleeping giant mill, 41th annual meetings of the Canadian metallurgical quarterly, vol. 47, no 3, pg. 277-284.
- [9] Kick, F., (1885). "das gesetz der proportionalen widerstande", pub. By Arthur Felix, Leipzig, Germany
- [10] Rajamani, R. K., Mishra, b. K., Venugopal, R. and Datta, A., (2000). Discrete element analysis of tumbling mills. *Powder technology*, **109**, pp. 105-112.
- [11] Taggart, A.F., "Handbook of mineral dressing", John Wile and Sons, Inc., N.Y., sec. 5, p.126 (1945).
- [12] von Rittinger P. R.: *Lehrbuch der Aufbereitungskunde*. Berlin, 1867.